

Rashba effect in 2D mesoscopic systems with transverse magnetic field

S. Bellucci¹ and P. Onorato^{1,2}

¹INFN, Laboratori Nazionali di Frascati, P.O. Box 13, 00044 Frascati, Italy.

²Dipartimento di Scienze Fisiche, Università degli Studi di Napoli "Federico II", Via Cintia, I-80126 Napoli, Italy.

(November 12, 2018)

We present semiclassical and quantum mechanical results for the effects of a strong magnetic field in Quantum Wires in the presence of Rashba Spin Orbit coupling. Analytical and numerical results show how the perturbation acts in the presence of a transverse magnetic field in the ballistic regime and we assume a strong reduction of the backward scattering interaction which could have some consequences for the Tomonaga-Luttinger transport. We analyze the spin texture due to the action of Spin Orbit coupling and magnetic field often referring to the semiclassical solutions that magnify the singular spin polarization: results are obtained for free electrons in a twodimensional electron gas and for electrons in a Quantum Wire. We propose the systems as possible devices for the spin filtering at various regimes.

71.10.Pm, 72.10.-d, 73.23.-b

I. INTRODUCTION

Recently the idea to use the electron spin in mesoscopic devices has generated a lot of interest and the "spintronic" opens new perspectives to semiconductor device technology and to quantum computation. In quantum computation the electron spin plays a central role and offers unique possibilities in order to find new mechanisms for information processing and information transmission¹⁻³. Datta and Das⁴ describe how the electrical field can be used to modulate the current: essential for this mechanism is the field-dependent Spin Orbit(SO) coupling.

The SO interaction has an essentially relativistic nature because it stems directly from the quadratic in v/c expansion of the Dirac equation⁵. However, this perturbation can give rise to a sensible modification of a semiconductor band structure^{7,8}.

The effects of an electric field on a moving electron have to be analyzed starting from the SO hamiltonian

$$\hat{H}_{SO} = -\frac{\hbar}{(2M_0c)^2} \mathbf{E}(\mathbf{R}) \left[\hat{\sigma} \times \left\{ \hat{\mathbf{p}} + \frac{e}{c} \mathbf{A}(\mathbf{R}) \right\} \right]. \quad (1)$$

Here M_0 is the free electron mass, $\hat{\mathbf{p}}$ is the canonical momentum operator, $\hat{\sigma}$ are the Pauli matrices, $\mathbf{E}(\mathbf{R})$ is the electric field, $\mathbf{A}(\mathbf{R})$ is the vector potential, and \mathbf{R} is the 3D position vector.

The potential energy $V(\mathbf{r})$ now plays a central role because if we are able to modulate it we can construct a current modulator and a spin filter. In semiconductors heterostructures a natural SO coupling is always present because usually the mesoscopic low dimensional devices are made at GaAs/AlGaAs interface obtained by the MBE technology. In a triangular potential well at interface a *two dimensional electron gas* (2DEG) is entrapped: the interface electric field that accompanies the quantum-well asymmetry⁹ is directed along the normal to the device plane hence it can be the source of the potential energy $V(\mathbf{r})$ in eq.(1). Because of the small dimension of this well the electrons are fully confined in the

growth (z) direction, while their motion in the x-y plane is unrestricted.

Because it was first introduced by Rashba¹⁰ the mechanism of the SO interaction originating from the interface field is known as Rashba effect. When 2DEG is confined in a simple triangular well¹¹ along the z direction by the interface electric field $\vec{E} = (0, 0, E_z)$ the hamiltonian (1) becomes

$$\hat{H}_{SO} = \frac{\alpha}{\hbar} E_z M_0 (\sigma_x V_y - \sigma_y V_x) \quad (2)$$

where \mathbf{V} is the *velocity* $\mathbf{V} = \mathbf{p} + \frac{e}{c} \mathbf{A}(\mathbf{R})$ and corresponds to momentum if there is no external magnetic field. Experimentally, in GaAs-AsGaAl interface, one typically observes⁸ values for αE_z on the order of 10^{-11} eV m. The SO coupling due to the electric field in the z direction is stronger than the Zeeman term of interaction connected to a magnetic field acting on the system because of the strong reduction of the effective electron mass ($m^* = 0.068m_0$). The Zeeman spin splitting term is $g^* \mu_B B$ where g^* is the effective magnetic factor for electrons in this geometry (very low in GaAs) and μ_B is the Bohr magneton with the bare mass. So the mass renormalization reduces by 10 order the SO coupling and by 100 the Zeeman spin splitting.

In this paper we discuss what happens when a strong transverse magnetic field acts on a Quantum Wire (QW) in the presence of a Rashba coupling. First we show a simple semi-classical approach that suggests two possible mesoscopic devices for the spin filtering, then we discuss the effects of a magnetic field on the subbands structure of a Quantum Wire^{12,13} and show the complex spin topology by analyzing the detailed spin textures of the electron states¹⁴. The transport in QWs is connected to three different regimes, the two ones at very low temperatures correspond to the typical single electron tunneling (Coulomb blockade) and to Ballistic Transport (where the Landauer-Büttiker formalism applies)¹⁵ while, when the correlation is strong, the Tomonaga-Luttinger¹⁶⁻¹⁸ liquid regime dominates and the broken simple $k, -k$

symmetry gives a subband structure rather similar to the one of Single Wall Nanotubes. We suppose that a possible effect of the magnetic field is the back-scattering suppression due to the localization of the different channels on the two different edges of the device.

II. QUANTUM AND SEMI-CLASSICAL APPROACH

We discuss some general effects of an electric field on a classical charge particle in two dimensions with an intrinsic magnetic momentum μ . The dynamics in the presence of external fields suggests some applications in the selection of particles with polarized spin.

The simplest physical system consists of a free particle moving with initial momentum $\mathbf{p}_0 = m\mathbf{v}_0$ in the plane. Using eq.(2) in absence of magnetic field the total hamiltonian is

$$H = \frac{\mathbf{p}^2}{2m} + \gamma E_z (\mu \wedge \mathbf{p}) \rightarrow E = \frac{mv_0^2}{2} + \gamma E_z mv_0 \mu \sin(\vartheta) \quad (3)$$

while the corresponding Hamilton equations are $\dot{\mathbf{p}} = 0$, $\dot{\mathbf{x}} = \mathbf{v}_0(1 + \gamma E_z m \mu \sin(\vartheta))$. The difference between the unperturbed velocity \mathbf{V} and the real velocity $\dot{\mathbf{x}}$ plays a central role in the analysis of the scattering at Wire-lead interface as we show in section IV. A beam of classical particles with fixed \mathbf{p} is divided by an electric field in different beams with different speed (depending on the angle ϑ between μ and \mathbf{p}). This could be the mechanism for a *Time Of Flight filter* which uses the different time that particles with different magnetic moments employ to cross the same distance.

Besides this is the Rashba effect in quantum Mechanics. The Rashba quantum effect is due to the quantization of the magnetic momentum $\mu = \mu_0 \sigma$ so that each beam with definite momentum $\mathbf{p} = \hbar \mathbf{k}$ is split in two beams corresponding to the two opposite spin polarizations in the plane. The linear momentum $\mathbf{p} = \hbar \vec{k}$ commutes with the free electron hamiltonian, thus we obtain the modified spectrum in terms of $k = |\vec{k}|$

$$\varepsilon_{f.e.}^{\pm}(k) = \frac{\hbar^2(k \pm k_R)^2}{2m} - \frac{\hbar^2 k_R^2}{2m} \quad (4)$$

where $k_R^0 = \frac{m\alpha E_z}{\hbar} = \frac{v_R}{\hbar}$ is called Rashba wavevector and estimates the strength of the splitting. The wavefunctions corresponding to the hamiltonian $\hat{H}_0 + \hat{H}_{SO}$ are free waves in the orbital part while the spinor is quantized along the direction orthogonal to the motion. For $\mathbf{k} \parallel \hat{y}$ and $\mathbf{E} \parallel \hat{z}$

$$\phi_{k,s_x}(y) = \frac{e^{iky}}{\sqrt{2\pi L}} \chi_{s_x}^x.$$

The spinors are in the x -base: $\hat{\sigma}_x \chi_{\pm}^x = \pm(\hbar/2)\chi_{\pm}^x$ so that we define $\hat{\sigma}_{\pm} = 1/\sqrt{2}(\hat{\sigma}_y \pm i\hat{\sigma}_z)$.

Now we want show a simple semi-classical way to calculate the spin polarization. We start from the classical solution of the classical Hamilton (or Lagrange) equations, so we rewrite the perturbative hamiltonian as follows (see appendix A):

$$\hat{H}_{SO} = \frac{\alpha E_z M_0}{2} \begin{pmatrix} V_y(t) & -V_x(t) \\ -V_x(t) & -V_y(t) \end{pmatrix}, \quad (5)$$

which then we can diagonalize in order to obtain an energy correction and time dependent spinors. If we start from the simple straight motion along the \hat{y} axis we have $\mathbf{V}(t) = V_0 \hat{y}$ so that the splitting energy is $\Delta = \frac{\alpha E_z M_0 V_0}{2} = \frac{\alpha E_z \hbar k}{2}$. The spinors that correspond to the eigenvalues of eq.(5) are the unperturbed χ_{\pm}^x .

An interesting case is the one of a particle in circular motion: $V_x(t) = -\omega R \sin(\omega t)$ $V_y(t) = \omega R \cos(\omega t)$ where ω is the angular velocity and R the orbit radius. The energy splitting reads $\Delta = \frac{\alpha E_z M_0 \omega R}{2} = \frac{\alpha E_z \sqrt{M_0 \omega L_z}}{2}$. Now the spinors are time dependent and the mean values of the observables are $\langle \hat{\sigma}_x(t) \rangle = \pm \sigma_0 \cos(\omega t)$ $\langle \hat{\sigma}_y(t) \rangle = \pm \sigma_0 \sin(\omega t)$. They correspond to a spin precession at any time orthogonal to the vector $\mathbf{V}(t)$. In Fig.(1) we show the spin polarizations obtained from a semiclassical analysis.

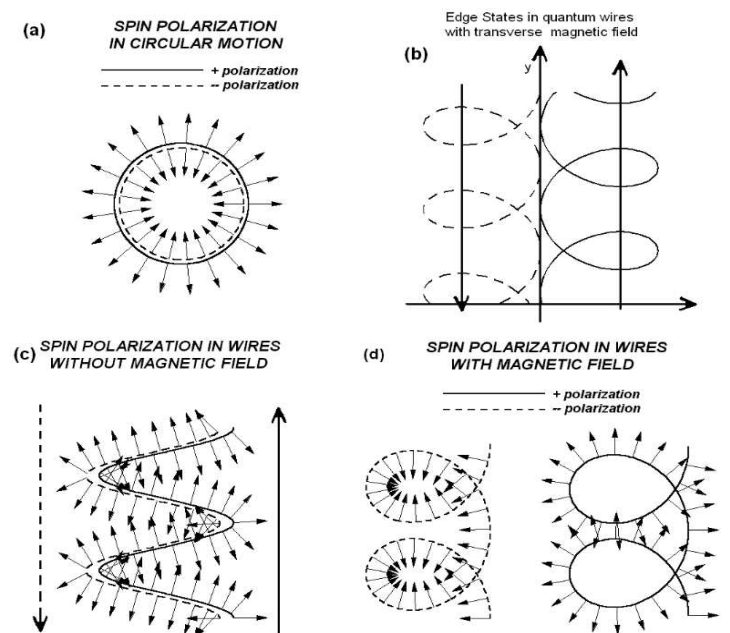


FIG. 1. Semiclassical spin textures for different orbits: a) spin polarization in circular motion; b) classical edge states in a Wire under the effect of a transverse magnetic field; c) spin polarization in a Wire without magnetic field; d) spin polarization for the edge states.

The case of an electron in a magnetic field directed

along the \hat{z} axis is quite similar to the one discussed here, when we consider the cyclotron frequency as the angular velocity $\omega_c = \frac{eB}{mc}$. Quantum Mechanical effects of the Rashba hamiltonian on a free charge under the action of a magnetic field are also discussed in the Appendix B.

III. QUANTUM WIRE

A Quantum Wire is usually defined by a parabolic confining potential along one of the directions in the plane: $V(x) = \frac{M_0}{2}\omega_d^2 x^2$. We also consider a uniform magnetic field B along the \hat{z} direction which allows a free choice in the gauge determination. We choose the gauge so that the system has a symmetry along the \hat{y} direction: $\mathbf{A} = (0, Bx, 0)$.

$$H_{n.w.} = M_0 \frac{V^2}{2} + \frac{M_0 \omega_d^2}{2} x^2 + \frac{\alpha}{\hbar} E_z M_0 (\sigma_x V_y - \sigma_y V_x) \quad (6)$$

where $M_0 V_y = p_y - eBx/(M_0 c)$ and $M_0 V_x = p_x$. This system has also interesting limits: if we put to zero the magnetic field we have a simple narrow Wire¹⁴ while if also ω_d vanishes we have a free electron as in the case discussed in the previous section. If we let only ω_d go to 0 we obtain the electron in a uniform magnetic field in transverse gauge and the spectrum has to compare to the one found in the Appendix B by using a different gauge.

A. Semi-classical solution

In order to solve the hamiltonian in Quantum Wires we introduce the total frequency $\omega_T = \sqrt{\omega_d^2 + \omega_c^2}$ and point out that $p_y = V_y + eBx/(M_0 c)$ commutes with the hamiltonian

$$H_{n.w.} = \frac{\omega_d^2}{\omega_T^2} \frac{p_y^2}{2M_0} + \frac{p_x^2}{2M_0} + \frac{m\omega_T^2}{2} (x - x_0)^2 + H_{S.O.}, \quad (7)$$

where $x_0 = \frac{\omega_c p_y}{\omega_T^2 M_0}$. The classical Hamilton equations give us the orbital motion in the special case of vanishing $\dot{x}(0)$

$$\begin{aligned} x(t) &= x_0 + R \cos(\omega_T t) \\ y(t) &= V_d t - \frac{\omega_c}{\omega_T} R \sin(\omega_T t) + y(0) \end{aligned} \quad (8)$$

where the drift velocity $V_d = \frac{\omega_d p_y}{\omega_T^2 M_0}$. We obtain $p_y = M_0(\dot{y}(0) + \omega_c x(0))$, $y(0) = 0$ and $R = x(0) - x_0$ from the boundary conditions. The two different motion along the Wire are localized on the two different edges as we can argue from the introduction of $\pm p_y \rightarrow \pm V_d$. These are also known in quantum mechanics as *edge states*.

It's impossible to find an exact solution of the perturbed hamiltonian as we can show by writing the usual semi-classical approximation for the energy splitting: in

this case the splitting energy depends on time and oscillates between two values

$$\Delta = \pm \frac{pR}{2} \sqrt{\Sigma V^2 + 2V_d \omega_c R \cos(\omega_T t) - R^2 \omega_d^2 \cos^2(\omega_T t)},$$

where $\Sigma V^2 = (V_d^2 + \omega_T^2 R^2)$. In Fig.(2) we show how the perturbation affects the dispersion law for vanishing magnetic field and strong SO coupling. Obviously there are no deviations from "parabolicity". As we show in the next subsection the subband deformation (Fig.(5)) is a second order quantum effect due to the crossing between two nearest subbands with opposite spin polarization. So in the classical case where no subbands can exist the Rashba effect is as usual.

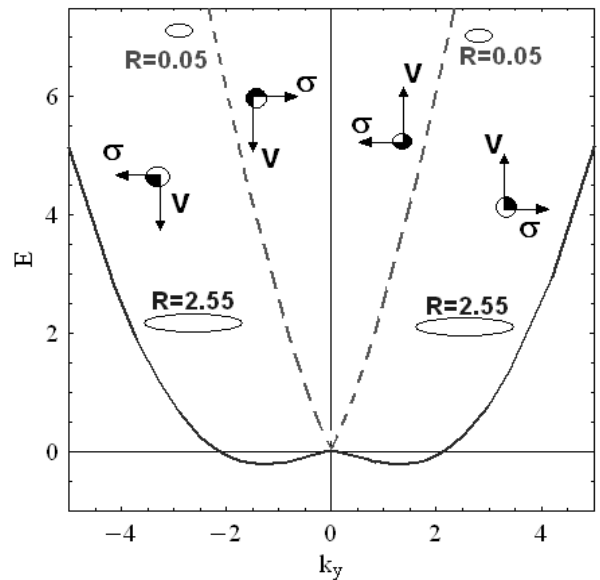


FIG. 2. Semiclassical dispersion law obtained from the energy after a mean value calculation. We show how the typical two split parabolas have to be constructed starting from solutions with $\pm\Delta$ but with different oscillations amplitude ($R_+ \neq R_-$). The semiclassical solutions give the dispersion law for a spin forming a definite angle ($\pm\pi/2$) with the velocity, while if we use the simple approach in the first section we have two parabolas with definite spin along the x axis.

Now we need some prediction about the spin polarization induced by the Rashba hamiltonian. Thus we can use the general formula eq.(A2) in Appendix A and calculate the spin polarization depending on time. Obviously this result (showed in Fig.(1)) cannot be matched with Quantum Mechanical calculations and we have to calculate the value of the spin component depending on coordinates or on momenta. So if we put $V_y = p_y/M_0$ and $V_x^2 = \omega^2(R^2 - x^2)$ we have

$$\langle \hat{\sigma}_x(x, p_y) \rangle = - \frac{p_y}{\sqrt{p_y^2 + M_0^2 \omega^2 (R^2 - x^2)}}.$$

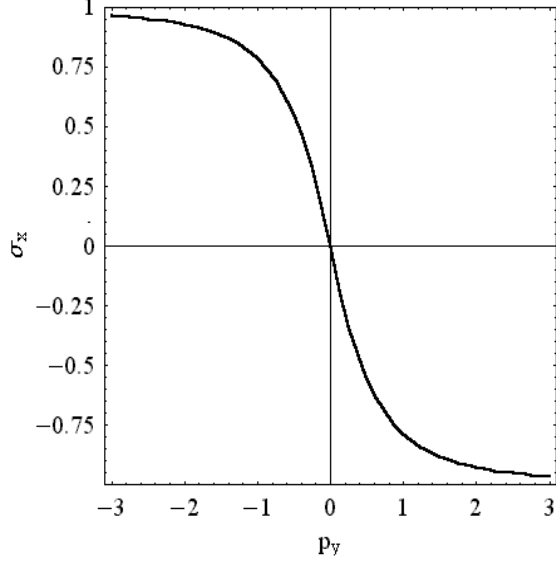


FIG. 3. Expectation value of the spin projection onto the x direction depending on momentum p_y .

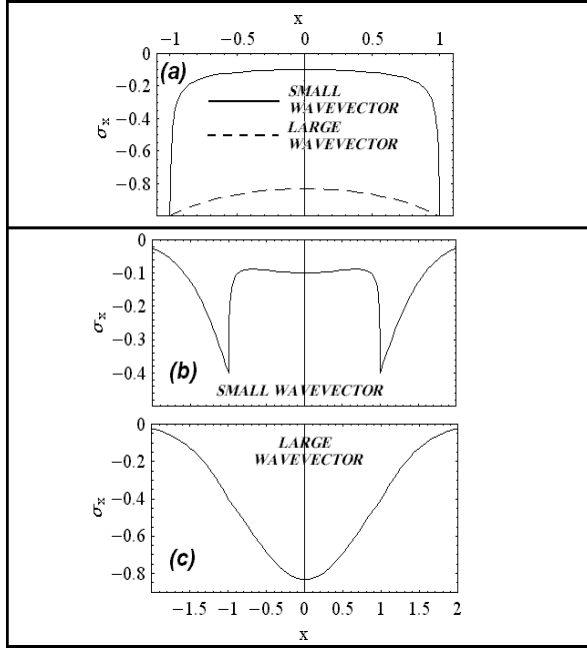


FIG. 4. Texture-like structure of the spin density across a Quantum Wire, calculated within the semiclassical approach. a) Spin density along x for large and small momenta. b) and c) Results analogous to those by Governale and Zulicke obtained by introducing a gaussian modulation of the spin density. All results were obtained without magnetic field.

The derivation of $\langle \hat{\sigma}_x(p_y) \rangle$ is obtained by integrating in x between $-R$ and R . The results agree with Quantum calculations by Governale and Zulicke¹⁴ as we show

in Fig.(3) that confirms conclusions reached in our previous discussion about the spin structure. We can also introduce a Gaussian correction which corresponds to the Quantum harmonic oscillations simply by multiplying $\langle \hat{\sigma}_x(x, p_y) \rangle$ by $\exp[-\frac{\omega M_0 x^2}{\hbar}]$ as showed in Fig.(4.b-4.c) and compare Semiclassical results with corresponding Quantum ones for small and large momenta (Fig.(4.a-4.b-4.c)).

B. Quantum Mechanical solution

As we know from the semiclassical approach the perturbed Quantum Wire has no exact solution and we can calculate its spectrum (and related wavefunctions) by a numerical calculation or with simple perturbation theory.

In order to introduce our result we can analyze the hamiltonian eq.(2) in the general case and separate the commuting part (which gives an exact solution)

$$\hat{H}_c = \frac{\alpha}{\hbar} E_z (p_y - M_0 \omega_c x) \hat{\sigma}_x = \frac{2p_R}{\hbar M_0} \hat{\sigma}_x (p_y - M_0 \omega_c x) \quad (9)$$

and the real perturbation

$$\hat{H}_n = \frac{\alpha}{\hbar} E_z p_x \hat{\sigma}_y = p_R \sqrt{\frac{2\omega_T}{M_0 \hbar}} (\hat{a} - \hat{a}^\dagger) (\hat{\sigma}_+ + \hat{\sigma}_-) \quad (10)$$

The first order approximation has no contributions from \hat{H}_n and gives us the usual result with a linear k -dependence that generates the Rashba subbands splitting

$$H_{I^0} = \frac{\omega_d^2}{\omega_T^2} \frac{(p_y - s p_R)^2}{2M_0} - \frac{\omega_d^2}{\omega_T^2} \frac{p_R^2}{2M_0} + \frac{p_x^2}{2M_0} + \frac{M_0 \omega_T^2}{2} (x - \xi_0^s)^2,$$

where $\xi_0^s = \frac{\omega_c (p_y - s p_R)}{\omega_T^2 M_0}$ and $s = \pm 1$ correspond to χ_\pm spin eigenfunctions. Hence the energies in the first order approximation read

$$\varepsilon_{n,k,s} = \hbar \omega_T (n + \frac{1}{2}) + \frac{\omega_d^2}{\omega_T^2} \frac{\hbar^2}{2M_0} ((k \pm k_R)^2 - k_R^2) \quad (11)$$

From the first order approximation we can conclude that 4-split channels are present in the Quantum Wire corresponding to $\pm p_y$ and $s = \pm 1$. When a magnetic field is present the usual energy and spin splitting¹² correspond to the different localization of the two channels and two different drift velocities.

If we set the Fermi level at energy E_F we find 4 Fermi momenta and related channels.

We can also observe that the distance between two different channels increases with the magnetic field strength and has an upper bound at $\delta \xi = 2 \sqrt{\frac{2E_F}{M_0}}$.

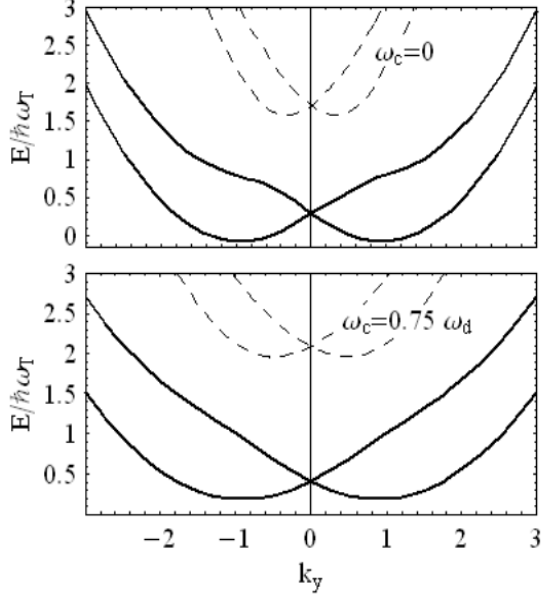


FIG. 5. Lowest and first excited spin-split subbands of a Quantum Wire, defined by a parabolic confining potential with oscillator in a 2D electron system, with strong Rashba SO coupling such that $p_R = 1$. We compare the two different cases of a vanishing magnetic field and a magnetic field of the same order of the oscillator strength $\omega_c = .75\omega_d$. As discussed in the text the crossing momentum increases with the magnetic field as $k_y^c \propto (1 + \frac{\omega_c^2}{\omega_d^2})^{\frac{3}{2}}$.

We cannot apply straightforwardly perturbation theory because of the crossing of the different subbands. From eq.(11) we can conclude that for $k_y^c = \pm \frac{M_0\omega_T^3}{2p_R\omega_d^2}$ the two states connected by the hamiltonian (10) are degenerate and a strong deformation (the so called avoided crossing) appears in the parabolic shape of the unperturbed subband. A numerical implementation allows us to take in account up to many subbands but the effect can also be seen in the simple 3 subband diagonalization. For the first subband we can limit us to a simple 2×2 matrix which represents the hamiltonian and we can give a simple analytical expression for the wavefunction and the mean values of the spin components.

It is possible to obtain a good quantitative description of the lowest spin-split subband by diagonalizing $H_{T0} + H_n$ in a truncated Hilbert space which is spanned by the lowest and first-excited parabolic subbands of the Hamiltonian as we discuss in Appendix C. In Fig.(4) we show the deviation from parabolicity, clearly visible near $\pm k_y^c$.

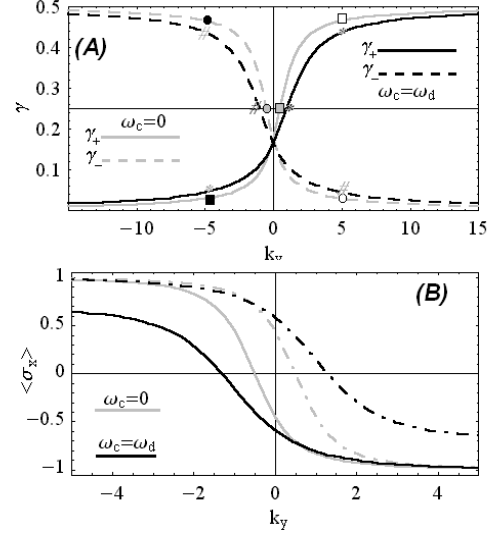


FIG. 6. Spin structure of electron states in a quantum Wire with strong SO coupling. A) γ angle as defined in Appendix C as a function of k_y for both zero and a strong magnetic field. B) Expectation value of the spin projection onto the x direction for electron states obtained in Fig.(5). Right-moving electrons with large wave vectors asymptotically have parallel spin which is opposite to that of the left-movers (dashing lines correspond to the left parabola in Fig.(5) while continuous ones correspond to the right parabola).

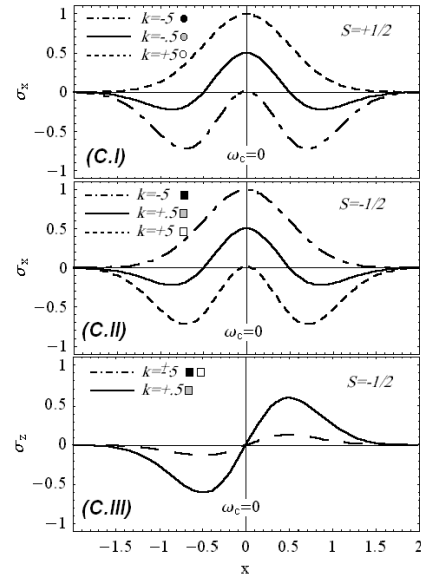


FIG. 7. Spin structure of electron states in a quantum Wire with strong SO coupling without magnetic field. Texture-like structure of the spin density across the Quantum Wire, calculated within the two-band model for the states indicated by dots and squares in Fig. (6.A). I) and II) Spatial variation of the x components of the spin density for the state with different wave vectors and in III) the z component.

In Fig.(6) and (7) we show some graphs useful in order to compare our results with those obtained by Governale and Zulicke Fig.(6.B) and Fig.(7) and we focus the effects of magnetic field in the system. In Fig.(8) the effects of localization are clearly showed in three different regimes. Large k_y of opposite signs correspond to the single state limit (*i.e.* γ is $\pi/2$ or vanishes as showed in Fig.(6.A)). The intermediate state corresponding to the k_y^c is a sum of the two states.

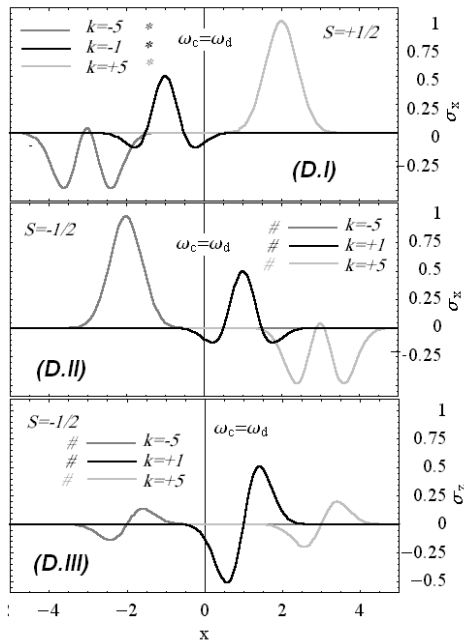


FIG. 8. Spin structure of electron states in a quantum Wire with strong SO coupling in the presence of a strong magnetic field ($\omega_c = \omega_d$). Texture-like structure of the spin density across the Quantum Wire, calculated within the two-band model for the states indicated by * and # in A). I) and II) Spatial variation of the x components of the spin density for the state with different wave vectors and in III) the z component.

IV. TRANSPORT

Now we apply the Landauer-Büttiker formalism^{19,20} and the Tomonaga-Luttinger^{21,22} model in order to discuss spin-dependent transport. These models correspond to two different regimes, one where we suppose that there is no electron-electron interaction (Ballistic conductance) and the opposite one where correlation effects due to the interaction dominate.

A. Non interacting electrons: Ballistic transport and Büttiker-Landauer formulation

A general model for near-equilibrium transport is due to the Landauer¹⁹ and Büttiker²⁰ contributions that are condensed in the so called Landauer formula. This formula expresses the conductance of a system at very low temperatures and very small bias voltages calculated directly from the energy spectrum by relating it to the number of forward propagating electron modes at a given Fermi energy

$$G \equiv G(\varepsilon_F) = \frac{e^2}{h} \sum_{\sigma, n} \sum_{\sigma', n'} |t_{\sigma, \sigma', n, n'}(\varepsilon_F)|^2, \quad (12)$$

where $t_{\sigma, \sigma', n, n'}(\varepsilon_F)$ are quantum mechanical transmission coefficients depending on the subband index and the spin. If we suppose $t_{\sigma, \sigma', n, n'} = \delta_{n, n'} \delta_{\sigma, \sigma'}$ we can limit ourselves to the number M of forward propagating electron modes at a given Fermi energy ε_F : $G = (e^2/h)M(\varepsilon_F)$.

In a Quantum Wire, if the width is smaller than the mean free path and comparable to the Fermi wavelength, the electrons move in a perfectly coherent way throughout the device *i.e.* the current can travel adiabatically in any state without scattering into any other one²³, so we can apply the ballistic theory.

Now we discuss the results obtained by Moroz and Barnes^{12,13} simply by counting the modes showed in Fig.(5). So we can point out the effects of the transverse magnetic field.

- In Fig.(5) we see a small *non-monotonic* portion (“bump”) in the energy curves $E(k_y)$ near k_y^c . Thus for the Fermi energy $\sim E(k_y^c)$ we have 3 propagating electron modes. Two of them have oppositely directed group velocities $v_y = \hbar^{-1}(\partial E/\partial k_y)$ so the effects on the conductance are damped. However the existence of such modes could give rise to sharp peaks in the conductance $G(E_F)$. The magnetic field shifts the peaks and also attenuates the effect.

- A second manifestation of the α -coupling is a shift of the conductance quantization steps by $\delta E = \frac{\omega_d^2 p_R^2}{2\omega_T^2 M_0}$ to lower energies, in comparison with the case of zero SO interaction. δE vanishes for a large magnetic field.

As discussed more recently by Governale and Zulicke¹⁴ the previous model could be not realistic because the SO coupling often vanishes in the contacts. In an hybrid system the transport is strongly affected by the scattering at Wire-lead interfaces due to the different nature of electron states in the Wire and the leads. The simplest model²⁴ is the one obtained by attaching semi-infinite leads with $p_R = 0$ to the Wire where $p_R \neq 0$. The transmission problem can be solved exactly by matching appropriate *Ansätze* for wave functions in the Wire and the leads. The usual condition for ensuring current conservation has to be modified because the semiclassical velocity

for electrons in the Quantum Wire^{25,26} is affected by the SO coupling and the magnetic field:

$$v_y = \frac{\omega_d^2 p_y}{\omega_T^2 M_0} - \omega_c x(t) + \frac{p_R \sigma_x(t)}{M_0} . \quad (13)$$

For a 1D Wire it is easy to calculate the usual transmission value at interface²⁵ in eq.(D1). This formula well approximates the first order behaviour of the system but it does not include the subband scattering which is strongly enhanced by the magnetic field.

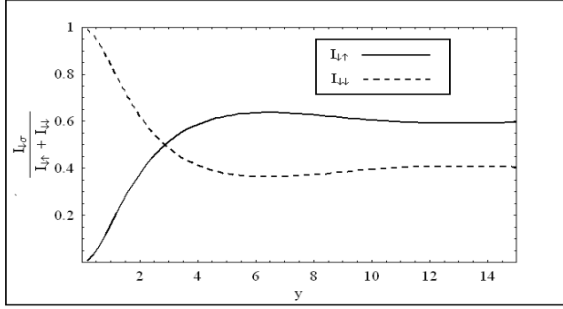


FIG. 9. Transport in a hybrid lead-Wire system (a semi-infinite Wire ($y > 0$) is attached to an ideal lead ($y < 0$)) calculated using the Landauer–Büttiker formalism. In the Wire a strong Rashba SO coupling is present: we show the conversion of incident spin-down current ($I_{\downarrow\sigma}$ denotes the spin- σ current in the Wire when a spin- \downarrow current is injected from the lead). We suppose $\gamma \approx \pi/3$, $p_R = .45$ and $k_0 \approx 1.3$ in the usual units ($M_0 = 1, \omega_d = 1, \hbar = 1$).

If the SO coupling is small ($p_R \ll \sqrt{\hbar M_0 \omega}$) we can limit ourselves to the analysis of the spin precession^{4,24} due to the Rashba hamiltonian. In this case we can limit ourselves to the first order perturbation with t_σ^0 and $H_{J\sigma}$. We conclude that a modulation of the transmitted current at drain appears when we inject a spin polarized current from the emitter to the Wire.

When the SO Coupling is very strong we have to turn to the two (or more) band model discussed in the previous section. In this case a current conversion is enabled by scattering into evanescent modes of the Wire, so that we have different behaviours in the current polarization close to the interfaces in the Wire and very far from it. We discuss all that in appendix D and we show the results in Fig.(9). In this figure we show the conversion of spin down incident current depending on the distance from the Wire-lead interface.

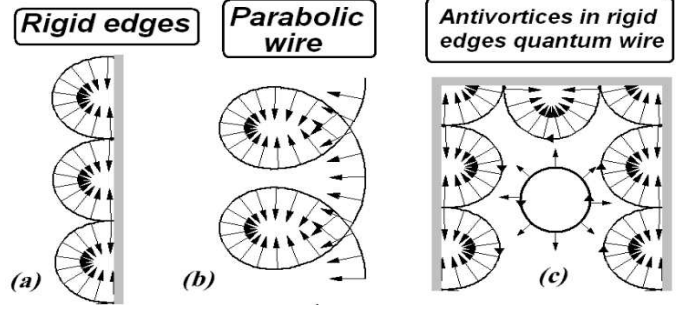


FIG. 10. In a) and b) we compare a rigid wells Wire and a parabolic one and give a heuristic explanation of the spin flip at the interface. In c) we show the mechanism for the current antivortices and the related spin polarization in the classical case.

1. Current and Spin vortices in Quantum Wires

When we consider the scattering of the current from the Wire-Lead interface (see Appendix D) we can have a very complex spin polarization related to the current. The presence of current antivortices in the Wire when the reflected current does not vanish is known (as the presence of vortices connected to the transmitted one²⁷) and can be easily explained in the classical case of a Wire with rigid wells Fig.(10). The antivortices are near the y axis if the transmission is very large, as we show in Fig.(11 and 12).

Normalized Current in the Wire

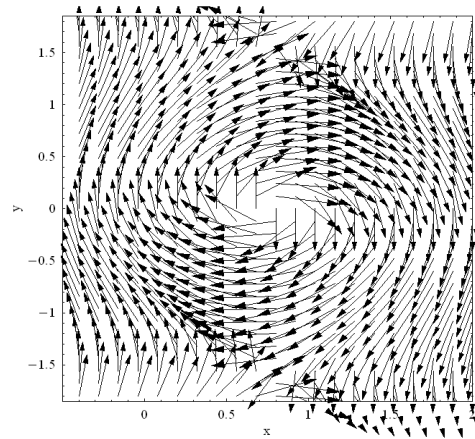


FIG. 11. We show the vector field of the current (eq.(D5)) renormalized with respect to its modulus around an antivortex. The antivortices go toward the y axis when the energy increases.

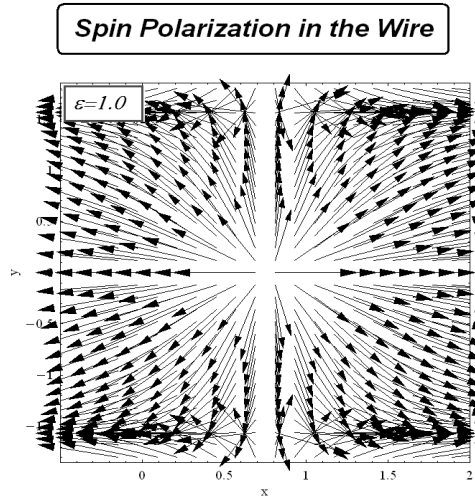


FIG. 12. We show the in plane spin texture near the antivortices. We can compare this texture with the one showed in Fig(10) for a rigid well wire and with the one in Fig.(1.a)

The quantum mechanical results, Fig.(11 and 12), confirm the classical picture giving a very singular spin texture all around the antivortices.

B. Interacting electrons: effective theory and Tomonaga-Luttinger model

As we discussed in the previous sections the strong effect of a magnetic field consists in the localization of the left and right going electrons on the opposite sides of the Wire. This effect correspond to a sort of 1-dimensionality suppression and reveals the 2-dimensional behaviour of the Wire. The magnetic field competes with the lateral confining potential in order to determine the exact dimension of the system. This could open new perspectives in the use of dimensional crossover²⁸⁻³¹ in order to analyze the Fermi-non Fermi liquid behaviour of interacting electrons in the Wire.

Next we refer to the usual approach to the Luttinger liquid in Quantum Wires under a strong Rashba SO coupling^{16,14,32}; this analysis is not in general correct for 1D systems but just for the limited class of semi-conducting Quantum Wires as discussed in Ref.¹⁸ where the Carbon Nanotube case is analyzed.

The effective low-energy description of an interacting quantum Wire starts from Tomonaga-Luttinger models²¹, so we have to linearize the single-electron energy spectrum close to the four Fermi points: we obtain two different electron velocities $v_{1,2} = \partial E(p_{1,2})/\partial p$ derived from the dispersion law in Fig.(5). Following Ref.¹⁶ we neglect Umklapp scattering, a legitimate assumption if the energy bands are far from being half-filled²², which is exactly the case, e.g., in Quantum Wires patterned in semiconductor heterostructures⁹.

In a future paper we intend to investigate the magnetic field effects on the Luttinger model parameters with some details. Now we just suppose that the magnetic field could improve the validity of the elimination of backward scattering especially when $\omega_c \approx \omega_d$ because of the localization of the edge states. In fact the distance between two electron with opposite momenta ($k_y, -k_y$) has a mean value increased by magnetic field as $\delta r \propto \frac{\omega_c}{\omega_T} k_y$. In the same way also forward scattering between electrons on the opposite branches (the usual g_2 coupling) is affected by the localization. So we can assume that a sort of chiral Luttinger liquid behaviour (where the non vanishing interaction parameter is just g_4) takes place in the Wire when the magnetic field is strong without the spin-charge separation.

So we can conclude as in Ref.¹⁶ that the SO coupling mixes together the charge and spin excitations and thereby destroys the usual spin-charge separation in the Tomonaga-Luttinger liquids.

Acknowledgement

This work is partly supported by the Italian Research Ministry, National Interest Program "Effetti di spin, interazione e proprietà di trasporto in sistemi elettronici fortemente interagenti a bassa dimensionalità".

APPENDIX A: GENERAL SOLUTION OF THE SEMI-CLASSICAL PROBLEM AND OBSERVABLES

Let us introduce the three spin operators $\hat{\sigma}_i$ in the x -based representation:

$$\hat{\sigma}_x = \frac{\hbar}{2} \begin{pmatrix} 1 & 0 \\ 0 & -1 \end{pmatrix}, \hat{\sigma}_y = \frac{\hbar}{2} \begin{pmatrix} 0 & 1 \\ 1 & 0 \end{pmatrix}, \hat{\sigma}_z = \frac{\hbar}{2} \begin{pmatrix} 0 & i \\ -i & 0 \end{pmatrix}$$

The Rashba hamiltonian in semi-classical approach is showed in eq.(5) and can be easily diagonalized giving the result:

$$\Delta\varepsilon_{\pm} = \pm \frac{p_R}{2\hbar^2} \sqrt{V_x(t)^2 + V_y(t)^2}. \quad (\text{A1})$$

which corresponds to an energy shift of the first order in p_R . The knowledge of the eigenvectors allows the calculation of the spin components

$$\begin{aligned} \langle \hat{\sigma}_x(t) \rangle &= \pm \frac{V_y(t)}{|\sqrt{V_x(t)^2 + V_y(t)^2}|} \\ \langle \hat{\sigma}_y(t) \rangle &= \mp \frac{V_x(t)}{|\sqrt{V_x(t)^2 + V_y(t)^2}|} \end{aligned} \quad (\text{A2})$$

In order to demonstrate that the spin polarization rotates we can solve the Hamilton equations to the first perturbative order. We start from the hamiltonian (2) and from the unperturbed orbits: $x(t), y(t), V_x(t), V_y(t)$.

Thus we introduce the hamiltonian equation at first order in p_R :

$$\begin{aligned}\dot{\sigma}_x &= \frac{p_R}{2} V_x \sigma_z \\ \dot{\sigma}_y &= \frac{p_R}{2} V_y \sigma_z \\ \dot{\sigma}_z &= \frac{p_R}{2} (V_y \sigma_y + V_x \sigma_x)\end{aligned}\quad (\text{A3})$$

It is simple to verify the general propriety: $[\dot{\sigma} \times \mathbf{V}]_z = 0$.

In order to solve eq.(A3) we can introduce a new spin vector rather similar to a polar one. So we introduce

$$\hat{\sigma}_{\parallel} = \frac{V_x \hat{\sigma}_x + V_y \hat{\sigma}_y}{\sqrt{V_x^2 + V_y^2}}, \hat{\sigma}_{\perp} = \frac{V_x \hat{\sigma}_y - V_y \hat{\sigma}_x}{\sqrt{V_x^2 + V_y^2}} \quad (\text{A4})$$

with the usual commutation rule $[\hat{\sigma}_{\parallel}, \hat{\sigma}_{\perp}] = i\hbar \hat{\sigma}_z$. So if we suppose that the orbits are unperturbed we obtain for the eq.(A3):

$$\begin{aligned}\dot{\sigma}_{\perp} &= 0 \\ \dot{\sigma}_{\parallel} &= \frac{p_R}{2} \sqrt{V_x^2 + V_y^2} \sigma_z \\ \dot{\sigma}_z &= -\frac{p_R}{2} \sqrt{V_x^2 + V_y^2} \sigma_{\parallel}\end{aligned}\quad (\text{A5})$$

These equations have a simple solutions if $\sqrt{V_x^2 + V_y^2}$ does not depend on time, with two oscillating components of the spin vector with frequency $\omega_p = \frac{p_R}{2} \sqrt{V_x^2 + V_y^2}$. However the first order correction to the energy correspond to that one in eq.(A1).

APPENDIX B: RASHBA EFFECT IN THE SYMMETRIC GAUGE

In this section we show the effect of a transverse magnetic field on a free electron when SO perturbation is also present. The difference with the calculation of Section III in the limit of vanishing potential ($V(x)$) is the different gauge that we choose. Thanks to this choice we can exactly solve the quantum problem. The symmetric gauge is $\mathbf{A} = (-By/2, Bx/2, 0)$ so that we can define:

$$\begin{aligned}V_x &= p_x + \frac{eBy}{2M_0c} & V_y &= p_y - \frac{eBx}{2M_0c} \\ V_+ &= \frac{1}{\sqrt{2}}(V_x + iV_y) & V_- &= \frac{1}{\sqrt{2}}(V_x - iV_y) \\ \hat{\sigma}_+^z &= \frac{1}{\sqrt{2}}(\hat{\sigma}_x + i\hat{\sigma}_y) & \hat{\sigma}_-^z &= \frac{1}{\sqrt{2}}(\hat{\sigma}_x - i\hat{\sigma}_y)\end{aligned}\quad (\text{B1})$$

The hamiltonian reads

$$H_0 + H_{SO} = \frac{M_0}{2}(V_- V_+ + V_+ V_-) + i\frac{p_R}{\hbar}(V_- \sigma_+ - V_+ \sigma_-).$$

From the commutation rules $[V_+, V_-] = \frac{\hbar\omega_c}{2M_0}$ we can deduce that V_{\pm} correspond to a_- an a_-^\dagger operators in the 2D isotropic harmonic oscillator. Hence we can rewrite the previous hamiltonian as follows:

$$\begin{aligned}H_0 + H_{SO} &= \hbar\omega_c(a_-^\dagger a_- + \frac{1}{2}) + \\ & i\frac{p_R}{\hbar} \sqrt{\frac{\hbar\omega_c}{M_0}}(a_-^\dagger \sigma_+ - a_- \sigma_-)\end{aligned}\quad (\text{B2})$$

where the angular momentum is given by $l_z = m = n_+ - n_-$ and n_- labels the Landau levels with energy $(n_- + \frac{1}{2})\hbar\omega_c$. The spin coupling term in eq.(B2) appears as a perturbation but can be also exactly diagonalized, because it connects just two nearest Landau Levels with the same value of $j_z = m + s_z = n_+ - n_- + s_z$. Therefore, also n_+ is an invariant.

The unperturbed wave-functions are

$$\psi_{k,m}^L(\vec{r}) = (\text{const.}) \exp(im\varphi) r^{|m|} \exp(-Br^2) L_k^{|m|}(2Br^2)$$

where $\vec{r} = (r \cos \varphi, r \sin \varphi)$ and $L_k^{|m|}$ is an associated Laguerre polynomial and $k = n_- - \frac{1}{2}(|m| - m)$. For sake of simplicity we choose $m > 0$. So we can start from the unperturbed eigenfunctions $\psi_{n_-, m}^L \chi_{\uparrow}^z = |n_-, n_+, \uparrow\rangle$ and the corresponding $j_z = (n_+ - n_-) + 1/2$ states $|n_- - 1, n_+, \downarrow\rangle$.

In this 2×2 subspace the hamiltonian eq.(B2) can be easily diagonalized with eigenvalues

$$\epsilon_{n_-, \pm}^{j_z, n_+} = n_- \hbar\omega_c \pm \sqrt{\left(\frac{\hbar\omega_c}{2}\right)^2 + \frac{p_R^2 \omega_c}{4M_0 \hbar} n_-}$$

while the lowest Landau level with spin up is not split. Finally we can introduce the perturbed wave functions as:

$$|n_-, \pm\rangle_{j_z, n_+} = \cos(\gamma_{\pm}) |n_- - 1, n_+, \downarrow\rangle + i \sin(\gamma_{\pm}) |n_-, n_+, \uparrow\rangle$$

where

$$\tan(\gamma_{\pm}) = -\frac{\frac{\hbar\omega_c}{2} \pm \sqrt{\left(\frac{\hbar\omega_c}{2}\right)^2 + \frac{p_R^2 \omega_c}{4M_0 \hbar} n_-}}{\sqrt{\frac{p_R^2 \omega_c}{4M_0 \hbar} n_-}}$$

Thus we can calculate the mean values of the spin components

$$\langle \sigma_x(r, \varphi) \rangle = F(r) \sin(2\gamma_{\pm}) \cos(\varphi) \quad (\text{B3})$$

$$\langle \sigma_y(r, \varphi) \rangle = F(r) \sin(2\gamma_{\pm}) \sin(\varphi) \quad (\text{B4})$$

where $F(r)$ is a radial function depending on n_- and n_+ easily obtained from the unperturbed wavefunctions.

APPENDIX C: TWO SUBBANDS ANALYTIC SOLUTION FOR THE LOWEST LEVEL IN A QUANTUM WIRE

We start from the spectrum in eq.(11) and we consider the effects on the ground states (GS) with opposite spin of the hamiltonian \hat{H}_n (10). If we chose the GS with spin up ($v_0 = |0, k_y, \uparrow\rangle$) the effect of \hat{H}_n is to increase the subband label and decrease the spin ($v_1 = |1, k_y, \downarrow\rangle$). In the matrix representation the total hamiltonian in the subspace ($\{v_0, v_1\}$) becomes

$$H = \left(\hbar\omega_T + \frac{\omega_d^2}{\omega_T^2} \frac{\hbar^2}{2M_0} k_y^2 \right) \begin{pmatrix} 1 & 0 \\ 0 & 1 \end{pmatrix} + \begin{pmatrix} a & ib \\ -ib & a \end{pmatrix} \quad (\text{C1})$$

where

$$a = \left(\frac{\hbar\omega_T}{2} + \frac{\omega_d^2}{\omega_T^2} \frac{\hbar k_y p_R}{M_0} \right), \quad b = p_R \sqrt{\frac{2\omega_T}{M_0 \hbar}},$$

so that we can easily diagonalize and obtain

$$\Delta\varepsilon = \sqrt{a^2 + b^2}, \quad \tan(\gamma_{\pm}) = \frac{a \mp \Delta\varepsilon}{b}.$$

So the new eigenvectors have the form:

$$\varphi = e^{ik_y y} \left(\cos(\gamma_{\pm}) u_{0,k_y,\uparrow}(x) \chi_{\uparrow}^x + i \sin(\gamma_{\pm}) u_{1,k_y,\downarrow}(x) \chi_{\downarrow}^x \right)$$

where $u_{n,k_y,\uparrow}(x) = \exp(x - \xi_0^s)^2 h_n(x - \xi_0^s)$ with ξ_0^s depending on k_y so that

$$\langle \hat{\sigma}_x(x, k_y) \rangle = \frac{\cos(\gamma_{\pm})^2 u_{0,k_y,\uparrow}(x)^2 - \sin(\gamma_{\pm})^2 u_{1,k_y,\downarrow}(x)^2}{\cos(\gamma_{\pm})^2 u_{0,k_y,\uparrow}(x)^2 + \sin(\gamma_{\pm})^2 u_{1,k_y,\downarrow}(x)^2}.$$

APPENDIX D: SIMPLE ANALYTICAL SOLUTION FOR THE LEAD-WIRE SCATTERING

In order to apply the Landauer formula we need a method to determinate the transmission and reflection coefficients for a given energy. So we have to solve the Schrödinger equation near the lead-Wire interface ($y = 0$).

The first step is the solution of the first order problem for the lowest subband ($n = 0$). Starting from eq.(11), we fix the Fermi energy and find the wavevectors in the Wire k_w and the lead k_L depending on the spin label s_x

$$k_w^s(\varepsilon_F) = s k_R \pm \sqrt{k_R^2 + k_0^2} \quad k_L(\varepsilon_F) = \pm k_0$$

where

$$k_0^2 = 2M_0 \frac{\omega_T^2}{\omega_d^2} \left(\varepsilon_F - \frac{\hbar\omega_T}{2} \right).$$

Next, we inject the electron with spin $s_z = 1/2$ corresponding to the spinor $\frac{1}{\sqrt{2}} \begin{pmatrix} i \\ 1 \end{pmatrix}$

$$\begin{aligned} & \frac{u_0(x)}{\sqrt{2}} e^{ik_0 y} \begin{pmatrix} i \\ 1 \end{pmatrix} + r_{\uparrow} u_0(x) e^{-ik_0 y} \begin{pmatrix} 1 \\ 0 \end{pmatrix} \\ & + r_{\downarrow} u_0(x) e^{-ik_0 y} \begin{pmatrix} 0 \\ 1 \end{pmatrix} \\ & + t_{\uparrow} u_0^{k,\uparrow}(x) e^{ik_w^{\uparrow} y} \begin{pmatrix} 1 \\ 0 \end{pmatrix} + t_{\downarrow} u_0^{k,\downarrow}(x) e^{ik_w^{\downarrow} y} \begin{pmatrix} 0 \\ 1 \end{pmatrix}. \end{aligned}$$

Then we introduce the conditions for the continuity of the wave function and the current flux ($-i\partial_y - p_R/m\hat{\sigma}_x$) at the interface. The simple case of vanishing magnetic field can be solved starting from the equivalence $u_0(x) =$

$u_0^{k,s}(x)$ and implies two identical systems of equations for \uparrow and \downarrow spins

$$t_{\uparrow}^0 = i t_{\downarrow}^0 = i \frac{\sqrt{2} k_0}{k_0 + \sqrt{k_0^2 + k_R^2}}. \quad (D1)$$

From these coefficients we can evaluate the mean value of $\hat{\sigma}_z$ and the probability of detecting a spin up (down) electron at the collector $P_{s_z=1}(y=L)$ at interface

$$\langle \hat{\sigma}_z \rangle = \frac{\cos(2k_R L)}{2} \quad P_{s_z=1} \propto \cos(k_R L)^2 \quad P_{s_z=-1} \propto \sin(k_R L)^2.$$

This is the basis of Datta and Das device for spin filtering.

The strong Rashba effect for vanishing magnetic field is just a little more difficult: we have to introduce the SO called evanescent states from the higher subbands while the transmitted states in the Wire are not any more pure $u_0(x)$ but the more complex function φ . If we are near the k_y^c energy just the \downarrow eigenfunction is affected by the second order perturbation while the \uparrow one is as in the previous case. Here we do not discuss the more complex case of non monotonicity discussed in the text so we have to modify the wavefunction in the Wire in a very simple manner

$$\begin{aligned} & t_{\uparrow} u_0(x) e^{ik_w^{\uparrow} y} \begin{pmatrix} 1 \\ 0 \end{pmatrix} + \tau_{\uparrow} u_1(x) e^{ik_R y - qy} \begin{pmatrix} 1 \\ 0 \end{pmatrix} + \\ & + t_{\downarrow} \left(\cos(\gamma) u_0(x) e^{ik_w^{\downarrow} y} \begin{pmatrix} 0 \\ 1 \end{pmatrix} + i \sin(\gamma) u_1(x) e^{ik_w^{\downarrow} y} \begin{pmatrix} 1 \\ 0 \end{pmatrix} \right) \end{aligned}$$

and also add a reflected evanescent channel in the lead

$$\rho_{\uparrow} u_1(x) e^{\chi_0 y}$$

where $\chi_0^2 = 2M_0 \frac{\omega_T^2}{\omega_d^2} \left(\frac{3\hbar\omega_T}{2} - \varepsilon_F \right)$ and $q^2 = \chi_0^2 + k_R^2$.

If we remember that $\langle u_0 | u_1 \rangle = 0$ we obtain three systems of equations corresponding to $\begin{pmatrix} 1 \\ 0 \end{pmatrix} u_0$, $\begin{pmatrix} 1 \\ 0 \end{pmatrix} u_1$, $\begin{pmatrix} 0 \\ 1 \end{pmatrix} u_0$ easily solvable in the coefficients. We also recall that no spin-polarized current is generated in the leads. So we can put $\rho_{\uparrow} = 0$ and obtain

$$t_{\uparrow}^I = t_{\uparrow}^0; \quad t_{\downarrow}^I = i \frac{t_{\uparrow}^0}{\cos(\gamma)} \quad \tau_{\uparrow}^I = \tan(\gamma) t_{\uparrow}^0 \quad (D2)$$

Now we can use the usual Büttiker-Landauer formulation^{19,20}. So we confirm the results about the spin polarization in Ref.¹⁴ as we show in Fig.(9). We have a generated spin-up current from an incident spin-down one

$$I_{\downarrow\uparrow} = k_{\Delta} (1 - e^{-qy} \cos[k_{\Delta} y]) \tan^2(\gamma) |t_{\uparrow}^0|^2$$

where $k_{\Sigma} = \sqrt{k_R^2 + k_0^2}$ and $k_{\Delta} = k_{\Sigma} - 2k_R$. The damped oscillations in the current vanish when the distance from the interface increases and we have a polarized current.

a. Reflection by a Wire-lead interface in the presence of a magnetic field

We can start from the spinless case of one electron reflected by an interface. We have to remember that in this case the wavefunctions are localized in the opposite edges of the Wire. The simple solutions of the previous section are now not the exact ones but we also use the simple 1D approach that could yield a good approximation. However is clear that, also in absence of spin, evanescent states have to be included in order to have an exact calculation of the transmission coefficients.

A fundamental step in our analysis is the definition of a correct *Ansatz* for the spin conservation in the scattering. If we compare the spin polarization in the edge states in a parabolic confined Wire Fig.(1.d) with the edge states reflected by rigid edges we can conclude that in the reflection from a rigid well the spin polarization is not conserved. We can show that the wedge product between velocity and spin is preserved as we show in Fig.(10). We suppose that the conserved quantity be $(\vec{\sigma} \times \vec{v})_z$ *i.e.* we have in the reflection

$$\vec{v} \rightarrow -\vec{v} \Rightarrow \vec{\sigma}_p \rightarrow -\vec{\sigma}_p \quad \sigma_z \rightarrow \sigma_z$$

where $\vec{\sigma}_p$ is the spin in the $x - y$ plane.

Now we calculate the one channel model corresponding to the incident $|k, \uparrow\rangle$ state, the reflected $r_\downarrow | -k, \downarrow\rangle$ and the transmitted $t_\uparrow | k_0, \uparrow\rangle$ state where $k = k_0 + k_R$. The reflection coefficient reads

$$r_\downarrow = \frac{k_R}{2k_0 + k_R} = e^{-2\Delta_R}.$$

Thus we can express the wavefunction in the Quantum Wire to first order as follows:

$$\begin{aligned} \psi(x, y) &= N e^{-\frac{(x^2 + \xi^2)}{2} - \Delta_R} \begin{pmatrix} e^{x\xi + \Delta_R} e^{iky} \\ e^{-x\xi - \Delta_R} e^{-iky} \end{pmatrix} \\ &= f(x) \begin{pmatrix} e^{x\xi + \Delta_R} e^{iky} \\ e^{-x\xi - \Delta_R} e^{-iky} \end{pmatrix}. \end{aligned} \quad (\text{D3})$$

Then we can calculate the density node as the value of x and y such that $\langle \psi^\dagger(x, y) | \psi(x, y) \rangle = 0$

$$x(\varepsilon_F) = -\frac{\Delta_R(\varepsilon_F)}{\xi(\varepsilon_F)} \quad y_n(\varepsilon_F) = -\frac{(2n+1)\pi}{2k(\varepsilon_F)}. \quad (\text{D4})$$

We can also get the current

$$\begin{aligned} j_x(x, y) &= 4f^2(x)\xi \sin(2ky) \\ j_y(x, y) &= -4f^2(x)k_0 \sinh(2x\xi + 2\Delta_R) \end{aligned} \quad (\text{D5})$$

and the spin

$$\begin{aligned} \langle \sigma_x(x, y) \rangle &= f^2(x) \sinh(2x\xi + 2\Delta_R) \\ \langle \sigma_y(x, y) \rangle &= f^2(x) \sin(2ky). \end{aligned} \quad (\text{D6})$$

From these formulae we can obtain the current vector field (which shows antivortices near the nodes of the

wavefunction Fig. (11) and Fig.(12)) and the spin texture with its very peculiar topology.

-
- ¹ B. E. Kane, Nature (London) **393**, 133 (1998); G. A. Prinz, Science **282**, 1660 (1998).
 - ² D. P. DiVincenzo, D. Bacon, J. Kempe, G. Burkard and K. B. Whaley, Nature (London) **408**, 339 (2000); D. Loss and D.P. DiVincenzo Phys. Rev. A **57**, 120 (1998) ; D. P. DiVincenzo Science **269**, 255 (1995).
 - ³ S. A. Wolf *et al.*, Science **294**, 1488 (2001).
 - ⁴ S. Datta and B. Das, Appl. Phys. Lett. **56**, 665 (1990).
 - ⁵ L. D. Landau, E. M. Lifshitz *Quantum Mechanics* (Pergamon Press, Oxford, 1991).
 - ⁶ G. P. Fisher, Am. J. Phys. **39**, 1528 (1971).
 - ⁷ H. L. Stormer, Z. Schlesinger, A. Chang, D. C. Tsui, A. C. Gossard, W. Wiegmann, Phys. Rev. Lett. **51**, 126 (1983).
 - ⁸ J. Nitta, T. Akazaki, H. Takayanagi, Phys. Rev. Lett. **78**, 1335 (1997).
 - ⁹ M. J. Kelly *Low-dimensional semiconductors: material, physics, technology, devices* (Oxford University Press, Oxford, 1995).
 - ¹⁰ E. I. Rashba, Fiz. Tverd. Tela (Leningrad) **2**, 1224 (1960) [Sov. Phys. – Solid State **2**, 1109 (1960)]; Yu. A. Bychkov, E. I. Rashba, Pis'ma Zh. Eksp. Teor. Fiz. **39**, 66 (1984) [JETP Lett. **39**, 78 (1984)].
 - ¹¹ For a review about the triangular well at the AsGa-As interface see T.J. Thornton, Rep. Prog. Phys. **58**, 311 (1995). For a discussion about the suppression of the Rashba field in nearly square quantum wells see T. Hassenkam, S. Pedersen, K. Baklanov, A. Kristensen, C. B. Sorensen, P. E. Lindelof, F. G. Pikus, G. E. Pikus, Phys. Rev. B **55**, 9298 (1997).
 - ¹² A. V. Moroz and C. H. W. Barnes, Phys. Rev. B **60**, 14272 (1999).
 - ¹³ A. V. Moroz and C. H. W. Barnes, Phys. Rev. B **61**, R2464 (2000).
 - ¹⁴ M. Governale, U. Zuelicke Phys. Rev. B **66**, 073311 (2002).
 - ¹⁵ C. W. J. Beenakker and H. van Houten *Quantum transport in Semiconductor Nanostructures*, vol. 44 of Solid state physics (Academic Press, New York, 1991).
 - ¹⁶ A. V. Moroz, K. V. Samokhin, and C. H. W. Barnes, Phys. Rev. Lett. **84**, 4164 (2000).
 - ¹⁷ A. V. Moroz, K. V. Samokhin, and C. H. W. Barnes, Phys. Rev. B **61**, R264 (2000).
 - ¹⁸ A. De Martino and R. Egger, Europhys. Lett. **56**, 570 (2001).
 - ¹⁹ R. Landauer, IBM J. Res. Dev. **1**, 223 (1957).
 - ²⁰ M. Büttiker, IBM J. Res. Dev. **32**, 317 (1988).
 - ²¹ S. Tomonaga, Prog. Theor. Phys. **5**, 544 (1950); J. M. Luttinger, J. Math. Phys. **4**, 1154 (1963); D. C. Mattis and E. H. Lieb, J. Math. Phys. **6**, 304 (1965).
 - ²² For a review see J. Sólyom, Adv. Phys. **28**, 201 (1979) and J. Voit, Rep. Prog. Phys. **57**, 977 (1994).
 - ²³ H. U. Baranger, A. D. Stone, Phys. Rev. B **40**, 8169 (1989).

- ²⁴ F. Mireles and G. Kirczenow, Phys. Rev. B **64**, 024426 (2001).
- ²⁵ L. W. Molenkamp, G. Schmidt, and G. E. W. Bauer, Phys. Rev. B **64**, 121202(R) (2001).
- ²⁶ U. Zülicke and C. Schroll, Phys. Rev. Lett. **88**, 029701 (2002).
- ²⁷ V. Marigliano Ramaglia F. Ventriglia and G. Zucchelli, Phys. Rev. B **48**, 2445 (1993).
- ²⁸ S. Bellucci and J. González, Eur. Phys. J. B **18**, 3 (2000).
- ²⁹ S. Bellucci and J. González, Phys. Rev. B **64**, 201106(R) (2001).
- ³⁰ S. Bellucci P. Onorato and J. González, , Nucl Phys. B 663 [FS] 605-621 (2003).
- ³¹ S. Bellucci P. Onorato and J. González, *Doping- and size-dependent suppression of tunneling in carbon nanotubes*, Phys. Rev. B (submitted), cond-mat/0304079.
- ³² W. Häusler, Phys. Rev. B **63**, 121310(R) (2001).